Juvenile Sportfish Monitoring in Florida Bay, Everglades National Park: Monitoring and Assessment Plan Results from 2004–2019

C. Kelble

J. Browder

C. Quenée-Stewart

I. Smith

K. Montenero

L. Visser

J. Contillo

Atlantic Oceanographic and Meteorological Laboratory
Miami, Florida

March 2021

U.S. DEPARTMENT OF COMMERCE

noaa

NATIONAL OCEANIC AND ATMOSPHERIC ADMINISTRATION
OFFICE OF OCEANIC AND ATMOSPHERIC RESEARCH

Suggested Citation

Acknowledgments

Disclaimer

Juvenile Sportfish Monitoring in Florida Bay, Everglades National Park: Monitoring and Assessment Plan Results from 2004–2019

Christopher R. Kelble[1]

Joan A. Browder[2]

Charline T. Quenée-Stewart[1,3]

Ian E. Smith[1,3]

Kelly A. Montenero[1,3]

Lindsey A. Visser[4]

Joseph P. Contillo[2]

[1]NOAA–Atlantic Oceanographic and Meteorological Laboratory
  Miami, Florida

[2]NOAA–Southeast Fisheries Science Center
  Miami, Florida

[3]University of Miami-Cooperative Institute for Marine and Atmospheric Studies
  Miami, Florida

[4]Broward County Environmental Monitoring Laboratory
  Davie, Florida

March 2021

Table of Contents

Figures

Tables

Acronyms

AOML   Atlantic Oceanographic and Meteorological Laboratory

BB   Braun-Blanquet abundance indices

CERP   Comprehensive Everglades Restoration Project

GLM   General linear model

HSI   Hyperspectral imaging

MAP   Monitoring and Assessment Plan

NOAA   National Oceanic and Atmospheric Administration

NSM   Natural system model

RECOVER   Restoration Coordination and Verification

SEFSC   Southeast Fisheries Science Center

Executive Summary

The spotted seatrout, *Cynoscion nebulosus*, is an important recreational sportfish in Florida Bay and spends its entire life history within the bay (Rutherford *et al.,* 1989). The geographic distribution of juvenile (20-100 mm standard length, 35-100 days old) *C. nebulosus* within the bay varies in response to salinity conditions, seagrass characteristics, and sediment types (Thayer and Chester, 1989). This and other findings clearly show that juvenile spotted seatrout are a good ecosystem indicator that is directly responsive to changes in freshwater runoff from the Everglades to Florida Bay. Plans to restore the Everglades are centered on continued increases in freshwater flows to Florida Bay in the future. These changes in freshwater flow are likely to impact sportfish populations in Florida Bay by affecting seatrout physiology and recruitment, as well as habitat, predator, and prey distributions.

This report describes reference conditions that can be used as a baseline to evaluate trends in juvenile spotted seatrout populations and compares current year juvenile spotted seatrout population metrics and environmental parameters with data sets from 2004-2019. The report describes juvenile abundance, as well as compares differences in abundance throughout the bay; examines the relationship between juvenile spotted seatrout abundance to salinity and seagrass habitat to provide insight into the potential response of spotted seatrout to Comprehensive Everglades Restoration Program (CERP) implementation; and determines salinity preferences for other juvenile sportfish in Florida Bay.

This project will help better predict juvenile sportfish responses to modifications in the timing, distribution, and quantity of freshwater inflow to Florida Bay and provide information to the adaptive management process on ecological effects in Florida Bay. Continued monitoring also provides insight on the effect of storms and other environmental events on sportfish distribution and abundance in Florida Bay. The effort to monitor juvenile sportfish in Florida Bay is a component of the Restoration Coordination and Verification (RECOVER) Monitoring and CERP Assessment Plan.

1. Introduction

The spotted seatrout, *Cynoscion nebulosus*, is an important recreational sportfish in Florida Bay and spends its entire life history within the Bay (Rutherford *et al.*, 1989). Spotted seatrout typically spawn multiple times between March and October at temperatures occurring between 27°C and 35°C (Powell, 2003). The geographic distribution of juvenile *Cynoscion nebulosus* (20-100 mm standard length, 35-100 days old) within the bay varies in response to salinity conditions, seagrass characteristics, and sediment types (Thayer and Chester, 1989). Western Florida Bay is an excellent habitat for juvenile spotted seatrout (Thayer *et al.*, 1987; Thayer and Chester, 1989). In 1984-1985, seatrout distributions were limited primarily to the western portion of the bay and absent from the north-central part of the bay, where hypersaline conditions prevailed. Hypersaline conditions are characteristic of the north-central sub-region of Florida Bay (Orlando *et al.*, 1997; Kelble *et al.*, 2007), although they are alleviated with increased freshwater inflow (Lee *et al.*, 2008), as the period of unusually high rainfall beginning in 1994 demonstrated. During 1994-1996, when hypersaline conditions in the north-central area of the bay were rare or absent, spotted seatrout juveniles expanded into the north-central part of the bay (Thayer *et al.*, 1999).

Powell (2003) reported substantial numbers of spotted seatrout larvae in Whipray Basin, a north-central sub-region of Florida Bay, from 1994-1999, but only in 1994 and 1995, a period of relatively low salinities, were there significant juvenile spotted seatrout populations here. Because of limited circulation from mudbanks (Fourqurean and Robblee, 1999), adults and juveniles are generally non-migratory, so larval distribution is a good indicator of spawning areas (Powell, 2003). These observations suggest spotted seatrout spawn viable eggs that produce larvae throughout Florida Bay; however, during hypersalinity, the larvae in the north-central sub-region likely fail to recruit into the juvenile population and thus never enter the adult population.

Salinity and freshwater influx affect spotted seatrout distribution both directly through physiology and indirectly by affecting habitat (i.e., seagrass), prey, and predator distributions and species compositions. Seagrass meadows are critical habitats for juvenile spotted seatrout (Chester and Thayer, 1990; Thayer *et al.*, 1999). Seagrass species are distributed unevenly throughout Florida Bay because of water depth, sediment depth, temperature, salinity, water clarity, and sediment organic content (Zieman *et al.*, 1989; Thayer and Chester, 1989). *Thalassia testudinum* is the dominant species in the bay, occurring most often on shallow mudbanks. *Syringodium filiforme* grows along the south and west portions of the bay in deeper areas of stronger oceanic influence, and *Halodule wrightii* is a pioneering species occurring in disturbed conditions (Zieman *et al.*, 1989).

Spotted seatrout occur more frequently in the western portion of the bay where a mixture of Syringodium and Thalassia is more prevalent because sediments are deeper with more organic content (Powell, 2003; Thayer and Chester, 1989). High densities of *Syringodium* and *Halodule* provide high quality juvenile spotted seatrout habitat, and areas of low seagrass diversity and density are areas where juvenile spotted seatrout are rare or absent (Thayer and Chester, 1989; Powell, 2003). *Thalassia* does not tolerate extreme fluctuations in salinity outside the minimum and maximum reported (10–48 ppt), and a major die-off of dense stands that occurred in the late 1980s was hypothesized to have been partially a result of hypersalinity (Fourqurean and Robblee, 1999). A *Thalassia* die-off in 2015 followed two consecutive years of low rainfall that led to an extreme hypersaline (defined as greater than ambient seawater salinity of 36.5 ppt) event in July 2015. High temperatures exacerbated salinity stress and decomposition of the dead grass, creating a low oxygen environment and a positive feedback loop that intensified and expanded the seagrass die-off.

Plans to restore the Everglades are centered on increasing freshwater flows to Florida Bay within the next few decades. Increased freshwater flows can have potential positive and negative impacts on spotted seatrout populations. Increased freshwater flows will alleviate hypersaline conditions, which are likely to allow an expanded distribution of the early life stages of spotted seatrout into the north-central part of the bay (Thayer *et al.*, 1999). There will be indirect effects as well, because the altered freshwater inflows will modify the current

seagrass distributions and seagrass species composition (Zieman *et al.*, 1989), as well as the distribution and species composition of both predators and prey of juvenile spotted seatrout. Increased predators could have a negative impact on juvenile spotted seatrout.

This project will help us better predict juvenile sportfish responses to modifications in the timing, distribution, and quantity of freshwater inflow to Florida Bay. But, because the realized effects of hydrologic restoration cannot be exactly known in advance due to interacting factors, species-specific responses, and species interactions, it is important to continue to monitor the juvenile seatrout and other juvenile sportfish as water management projects are implemented so that feedback on ecological effects in Florida Bay can be provided in the adaptive management process.

This project is a component of the Restoration Coordination and Verification (RECOVER) Monitoring and Assessment Plan of the Comprehensive Everglades Restoration Program (CERP). The objectives of this year's efforts were to: (1) develop reference conditions that can be used as a baseline to evaluate trends in juvenile spotted seatrout populations and, as an exercise, compare data with Monitoring and Assessment Plan (MAP) data sets (2004–2017); (2) develop a juvenile abundance index (mean density and frequency of occurrence) and determine if annual differences in abundance occur among areas in the bay; (3) examine the relationship between juvenile spotted seatrout abundance and salinity and use this analysis to gain insights into the potential response of spotted seatrout to CERP implementation; and (4) determine salinity preferences for other juvenile sportfish in Florida Bay.

2. Methods

2.1 Observational Data

The four sub-regions (**Figure 1**) in which spotted seatrout are monitored were selected based upon two criteria: (1) juvenile spotted seatrout were previously collected in the sub-region according to historical data; and (2) the sub-region is likely to be affected by water management

changes associated with CERP. Each sub-region was divided into cells (macrocells) measuring 1800 m per side, which were further divided into four smaller cells (microcells). Hence, there were four potential sampling sites per macrocell. Macrocells were randomly selected within each sub-region, and a microcell (900 m per side) was then randomly selected within the randomly selected macrocell. A sample was collected at the center of this microcell. Because of the presence of shallow mud banks, islands, and variable tides, many macrocells contained less than four trawlable microcells. If a microcell was unsuitable for trawling, another microcell within the macrocell was randomly chosen. If there were no suitable microcells within a macrocell, we randomly selected an alternate macrocell.

There are 50 trawlable macrocells in the West sub-region, 23 in Rankin, 19 in Whipray, and 20 in Crocodile Dragover (**Figure 1**). The sampling scheme from 2004 through 2008 was weighted by the number of trawlable sites per sub-region; therefore, the initial (through 2008) total number of samples to be collected annually (ca. 360) was distributed among the areas as follows: 156 samples per year in the West, 84 in Rankin, and 60 in both Whipray and Crocodile Dragover. A modified sampling distribution based on an updated power analysis (Cohen, 1988) began in 2009. This distribution collected 492 samples per year: 120 collected in the West; 138 in Rankin; 114 in Whipray; and 120 in Crocodile Dragover. In 2011, we again expanded the number of samples collected, this time to 140 samples in the West, 152 in Rankin, 134 in Whipray, and 140 in Crocodile Dragover for a total of 566 samples per year. This new sampling regime improved our ability to estimate the juvenile spotted seatrout population in the central areas of the bay, where the population is often low, but where the greatest change from CERP may occur.

Routine sampling is conducted monthly only from May through October (or through November when October status indicates November sampling would be productive), the period of peak abundance for juvenile spotted seatrout (Powell *et al.*, 2007). The annual sample total was divided equally for each month in each sub-region. The sampling design could not be completed every year. In 2004, funding did not become available until August, and
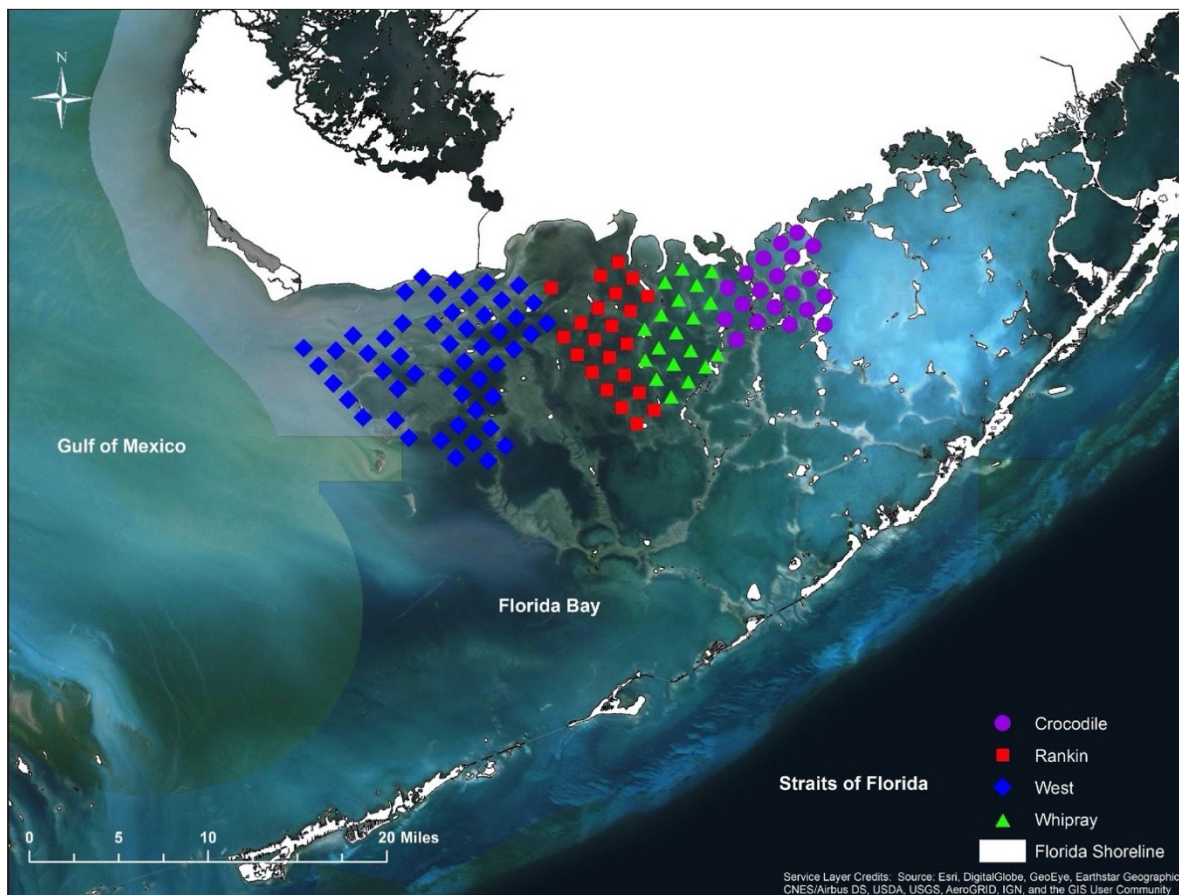
Figure 1. Locations of all potential sampling stations by sub-region in Florida Bay. Symbols are centered in the macrocell that is 1800 m per side.

a hurricane truncated sampling in September. In 2005, sampling was not performed in August, September, and only partially in October due to hurricanes. We sampled intensively in November 2005 in an attempt to reach our annual sampling goal. Sampling from 2006 through 2019 was as planned with minimal impact from adverse weather and funding delays. In 2017, winter sampling was added in the off-season from November through April after Hurricane Irma passed through South Florida to assess its effect on juvenile sportfish populations (Zink *et al*., 2020).

Juvenile spotted seatrout sampling was conducted with an otter trawl. The trawl has a 3.4 m head rope, 3.8 m footrope equipped with a 3 mm galvanized tickler chain, 6 mm mesh in the body, and a 3 mm mesh tail bag. The mouth opening has an effective width of 2.1 m. The trawl was towed at a speed of approximately 2.0 m s^{-1} for 2 min

(to sample an area of about 500 m^2), unless the net was clogged with detritus. If the net became clogged, the sample would be counted if the tow was longer than a minute or re-done if the clog occurred prior to 1 minute. In 2004-2007, a floating marker was deployed at the beginning and end of each tow and the distance between buoys measured using GPS technology (GPSMAP4212 and Garmin Homeport). In 2008, we modified this scheme, recording a waypoint in the GPS at the beginning and end of each tow to more accurately calculate the tow distance and bearing. The distance towed (calculated from the GPS waypoint) was multiplied by the mouth opening of the net to calculate the area sampled in a tow. Density (number of fish 1000 m^{-2}) and frequency of occurrence were calculated as the indices of abundance. Spotted seatrout <30 mm and >200 mm standard length were excluded from the analysis because the sampling gear did not effectively capture them. Although juvenile

spotted seatrout were the main target of our sampling, we also identified, measured, and counted all sizes of other species of sportfish caught in every tow. From a subset of 12 stations (five in West, two in Rankin, two in Whipray, three in Crocodile Dragover), for each month starting in 2009, all organisms under 100 mm total length found in the net were preserved in alcohol, then identified and measured in the lab for community and gut content analysis.

Temperature and salinity were measured with either a Hydrolab Scout 2 Water Quality Data System, a YSI environmental Professional 30 instrument (Pro30), a SeaBird Model 21 thermosalinograph, or an EXO2 multiparameter sonde at each tow. From 2009 through 2012, seagrass abundance was quantified by conducting triplicate Braun-Blanquet 0.25 m^2 quadrats at both endpoints and the midpoint of each tow and included estimates of macroalgal abundance. This was done to standardize our seagrass data collection with the Fisheries Habitat Assessment Program that monitors seagrass throughout Florida Bay. However, the Braun-Blanquet scale converts continuous percentages to discrete scores, making its utility for statistical analyses limited. Therefore, beginning in 2013, seagrass percent cover, to the nearest 5% value, was recorded for each quadrat instead of Braun-Blanquet abundance indices. A variety of statistical methods, including a non-parametric, Mann-Whitney U-test (Sokal and Rohlf, 1981) with $\alpha = 0.05$, were used for significance testing throughout the document and are briefly noted where used.

3. Results and Discussion

The frequency of occurrence and density (number 1000 m^{-2}) of juvenile *C. nebulosus* has been quantified for all years from 2004 through 2019 in which there was sampling in Florida Bay (16 years in total). Pre-MAP (i.e., pre-2004) sample sizes were small in each year (n < 15) and may not well represent the juvenile spotted seatrout population of a given year. Moreover, these Pre-MAP data were collected intermittently over 15 years in what is a dynamic environment and, therefore, is unlikely to accurately represent conditions throughout this 15-year

period. As such, we removed these data from our analyses and focused instead on the 2004 through 2019 data.

3.1 Monitoring Results: September 2004 through November 2019

In the West sub-region, 2019 had significantly greater densities of juvenile spotted seatrout than 2004, 2005, 2009, 2011, 2013, 2014, and 2015, but had significantly lower densities than 2006 (**Table 1**). Densities from 2007, 2008, 2010, 2012, and 2016-2018 were comparable to 2019 densities. However, 2006 had significantly higher densities of juvenile spotted seatrout than in all other years (**Figure 2**, **Table 1**). The frequency of occurrence was also highest in 2006 (0.45), but the frequency of occurrence has remained fairly stable over the past 4 years, with 2019 reporting at 0.24. The year 2019 had a significantly higher density than 2004, 2005, 2009, 2011, and 2013-2015. The year 2014 had a significantly lower density of juvenile spotted seatrout than all other years. In recent years, juvenile spotted seatrout densities in the West sub-region were much more consistent and generally higher than the rest of Florida Bay. As a result, 2006, 2016, 2017, 2018, and 2019 were deemed high-population years, while 2014 was the only low-population year, with all other years in the middle.

In Rankin, 2019 juvenile spotted seatrout densities were significantly higher than 2004 and 2008-2017 and not significantly lower than any other year (**Table 1**). The years 2005-2007 and 2018 were comparable to 2019 densities. Frequency of occurrence was highest in 2005 (0.39), but 2019 reported the second highest frequency of occurrence in monitoring history with (0.28). Juvenile spotted seatrout densities were significantly greater in 2004-2007 and 2016-2019 than in 2008-2015 (**Figure 2**, **Table 1**). The years 2004-2007 and 2016-2019 were thus deemed high-population years, and 2008-2015 were deemed low-population years for juvenile spotted seatrout in Rankin. Significant differences were present within these high-population years. Specifically, juvenile spotted seatrout density was significantly higher in 2005, 2006, and 2018 than in 2007 and 2016, and 2019 was significantly higher than 2004, 2016, and 2017. Within the low-population years, there were no significant differences (**Figure 2**, **Table 1**).

Table 1. Mann-Whitney U-test summary table of p-values comparing juvenile spotted seatrout densities between years within each sub-region. Arrows indicate if the year in the row was significantly higher or lower than the year in the column (i.e., in 2004, spotted seatrout density in the West was significantly lower than it was in 2006, 2016, 2017, 2018, and 2019, but higher than 2014).

Crocodile Dragover

Year	2004	2005	2006	2007	2008	2009	2010	2011	2012	2013	2014	2015	2016	2017	2018	2019
2004	---				↑			↑	↑	↑	↑	↑				↑
2005		---			↑		↑	↑	↑	↑	↑	↑	↑	↑		↑
2006			---					↑	↑	↑	↑	↑				↑
2007				---	↑		↑	↑	↑	↑	↑	↑				↑
2008	↓	↓		↓	---										↓	
2009						---		↑		↑	↑	↑				↑
2010		↓		↓			---								↓	
2011	↓	↓	↓	↓		↓		---							↓	
2012	↓	↓	↓	↓					---						↓	
2013	↓	↓	↓	↓		↓				---					↓	
2014	↓	↓	↓	↓		↓					---				↓	
2015	↓	↓	↓	↓		↓						---			↓	
2016		↓											---		↓	
2017		↓												---		
2018					↑		↑	↑	↑	↑	↑	↑	↑		---	↑
2019	↓	↓	↓	↓		↓									↓	---

Rankin

Year	2004	2005	2006	2007	2008	2009	2010	2011	2012	2013	2014	2015	2016	2017	2018	2019
2004	---	↓			↑	↑	↑	↑	↑	↑	↑	↑				↓
2005	↑	---		↑	↑	↑	↑	↑	↑	↑	↑	↑	↑	↑		
2006			---	↑	↑	↑	↑	↑	↑	↑	↑	↑	↑			
2007		↓	↓	---	↑	↑	↑	↑	↑	↑	↑	↑			↓	
2008	↓	↓	↓	↓	---								↓	↓	↓	↓
2009	↓	↓	↓	↓		---							↓	↓	↓	↓
2010	↓	↓	↓	↓			---						↓	↓	↓	↓
2011	↓	↓	↓	↓				---					↓	↓	↓	↓
2012	↓	↓	↓	↓					---				↓	↓	↓	↓
2013	↓	↓	↓	↓						---			↓	↓	↓	↓
2014	↓	↓	↓	↓							---		↓	↓	↓	↓
2015	↓	↓	↓	↓								---	↓	↓	↓	↓
2016		↓	↓		↑	↑	↑	↑	↑	↑	↑	↑	---		↓	↓
2017		↓			↑	↑	↑	↑	↑	↑	↑	↑		---		↓
2018				↑	↑	↑	↑	↑	↑	↑	↑	↑	↑		---	
2019	↑				↑	↑	↑	↑	↑	↑	↑	↑	↑	↑		---

West

Year	2004	2005	2006	2007	2008	2009	2010	2011	2012	2013	2014	2015	2016	2017	2018	2019
2004	---		↓								↑		↓	↓	↓	↓
2005		---	↓								↑		↓	↓	↓	↓
2006	↑	↑	---	↑	↑	↑	↑	↑	↑	↑	↑	↑	↑	↑	↑	↑
2007			↓	---							↑			↓		
2008			↓		---					↑	↑	↑				
2009			↓			---					↑		↓	↓	↓	↓
2010			↓				---				↑					
2011			↓					---			↑		↓	↓		↓
2012			↓						---		↑					
2013			↓		↓					---	↑		↓	↓	↓	↓
2014	↓	↓	↓	↓	↓	↓	↓	↓	↓	↓	---	↓	↓	↓	↓	↓
2015			↓		↓						↑	---	↓	↓	↓	↓
2016	↑	↑	↓			↑		↑			↑	↑	---			
2017	↑	↑	↓	↑		↑		↑			↑	↑	↑	---		
2018	↑	↑	↓			↑					↑	↑	↑		---	
2019	↑	↑	↓			↑		↑			↑	↑	↑			---

Whipray

Year	2004	2005	2006	2007	2008	2009	2010	2011	2012	2013	2014	2015	2016	2017	2018	2019
2004	---		↓	↓	↑		↑	↑			↑					
2005		---	↓		↑		↑	↑	↑	↑	↑	↑		↑		
2006	↑	↑	---	↑	↑	↑	↑	↑	↑	↑	↑	↑	↑	↑	↑	↑
2007	↑		↓	---	↑	↑	↑	↑	↑	↑	↑	↑	↑	↑		↑
2008	↓	↓	↓	↓	---										↓	↓
2009			↓	↓		---		↑	↑	↑	↑	↑	↑		↓	
2010	↓	↓	↓	↓		↓	---						↓	↓	↓	↓
2011	↓	↓	↓	↓		↓		---					↓		↓	↓
2012		↓	↓	↓		↓			---				↓		↓	↓
2013		↓	↓	↓		↓				---			↓		↓	↓
2014	↓	↓	↓	↓		↓					---		↓		↓	↓
2015		↓	↓	↓		↓						---	↓		↓	↓
2016		↓	↓				↑	↑	↑	↑	↑	↑	---		↓	↓
2017		↓	↓	↓			↑							---	↓	
2018			↓		↑	↑	↑	↑	↑	↑	↑	↑		↑	---	
2019			↓	↓	↑		↑	↑	↑	↑	↑	↑				---

Figure 2. Density (number 1000 m⁻² + standard error) as a bar chart with each error bar representing the standard error and frequency of occurrence as linked points for juvenile spotted seatrout by area and year in Florida Bay. Values in parentheses indicate the number of stations sampled.

In Whipray, a similar pattern followed: 2019 had significantly higher juvenile spotted seatrout densities than 2008 and 2010-2015, and significantly lower densities than 2006 and 2007 (**Table 1**). Densities from 2019 were similar to 2004, 2005, 2009, and 2016-2018. Frequency of occurrence was highest in 2006 (0.50), and 2019 frequency of occurrence (0.11) was in the middle of the range. The years 2004-2007, 2016, 2018, and 2019 had significantly higher juvenile spotted seatrout densities than 2008 and 2010-2015 (**Figure 2**, **Table 1**).

However, 2009, 2016, 2018, and 2019 had significantly higher population densities than 2010-2015, but lower densities than 2006. Thus, we deemed 2004-2007, 2016, 2018, and 2019 high-population years and 2008 and 2010-2015 low-population years, while 2009 and 2017 were in between these two groupings. Within the high-population years, 2006 had a significantly greater density than any other year (**Figure 2**, **Table 1**). Within the low-population years, there were no significant differences among years.

Crocodile Dragover typically followed a similar pattern to Whipray and Rankin for interannual changes in juvenile spotted seatrout density. The year 2019 was significantly lower than 2004-2007, 2009, and 2018 (**Table 1**). The years 2004-2007 had significantly greater juvenile spotted seatrout densities than most other years, including 2008 and 2010-2015 (**Figure 2**, **Table 1**). Frequency of occurrence was highest in 2005 (0.11) and, in 2019, it was among the lowest at (0.00). The year 2019 was not significantly different from 2008 and 2010-2017. Although mean density increased in 2016 and 2017, it was not significantly different from the low-population years and was still significantly lower than 2005 and 2007. The year 2018 showed a significant increase in mean density compared to most other years, but this increase disappeared in 2019. Thus, 2004-2007 and 2018 were deemed high-population years and 2008 and 2010-2015 were deemed low-population years.

The highest density and frequency of occurrence occurred in 2006 in Whipray basin and in the West region (**Figure 2**). In Whipray basin during September 2006, mean salinity was 30.7 and there were over six seatrout per 1000 m^{-2}. A notable increase in spotted seatrout densities in West and Rankin basins occurred in the fall of 2005, following a substantial decrease in salinity post-hurricanes (**Figure 3**). The lowest density and frequency of occurrence of seatrout was in 2014 when only two were caught the entire year in all sub-regions (452 stations sampled). The following year, 2015, had the second lowest number of seatrout caught for the sampling period at 3% of the stations (21 out of 482 stations). The year 2016 had a sharp increase in seatrout; they were caught at 10% of the stations (90 seatrout at 560 stations). Similarly, 2018 had the third highest frequency of occurrence, with spotted seatrout caught at 16.9% of stations (179 juvenile seatrout caught at 96 out of 568 stations). The highest annual frequency of occurrence was in 2006 when seatrout were caught at 34% of the stations (260 at 360 stations) (**Table 2**). The year 2019 showed increases in seatrout frequency of occurrence in both West and Rankin but decreases in Whipray and Crocodile Dragover. The overall frequency of occurrence was comparable to the previous year.

The West sub-region had one year of abnormally high juvenile *C. nebulosus* population in 2006 and one abnormally low year in 2014. The rest of the years in the West all varied from 9% to 24% frequency of occurrence for juvenile *C. nebulosus*, but the four most recent years were all over 20%, being the second, third, fourth, and fifth highest for the period of record. In the West sub-region, monthly patterns of juvenile spotted seatrout frequency of occurrence were variable, with a mean trend showing a decline at the end of May through November during all "normal" years (**Figure 3**). "Normal" years were defined as all years excluding high-population and low-population years. During the high population year of 2006, the peak frequency of occurrence occurred much later in September. In 2019, frequency of occurrence was just below the 25th quartile of high-population years for all years until October and November when it surpassed the 75th percentile of high-population years for both months. In 2019, frequency of occurrence in the West sub-region was 24% (33 stations with juvenile spotted seatrout present out of 140 stations).

In the Rankin sub-region, high-population years of 2004-2006 and 2017-2019 had frequencies of occurrence of 8% or higher. Low-population years of 2008-2015 all had a frequency of occurrence of 1% or less. In high-population years (2004-2007 and 2016-2019), seatrout frequency of occurrence generally increased during the sampling season, peaking in September through November and coinciding with a decrease in salinities in this sub-region during the sampling season (**Figures 3**, **4**, and **5**). During the low-population years, only a single seatrout was caught in Rankin in 2009, 2011, and 2013; none were caught in 2010, 2012, 2014, and 2015. Occurrence levels for four months of 2016 were within the same quartiles as the high-population years. In 2019, the frequency of occurrence in the Rankin sub-region was the second highest on record at 28% (43 stations with juvenile spotted seatrout present out of 154 stations). The monthly pattern of juvenile spotted seatrout frequency of occurrence in 2019 was started higher than other high-population years with a generally increasing trend throughout the sample period.
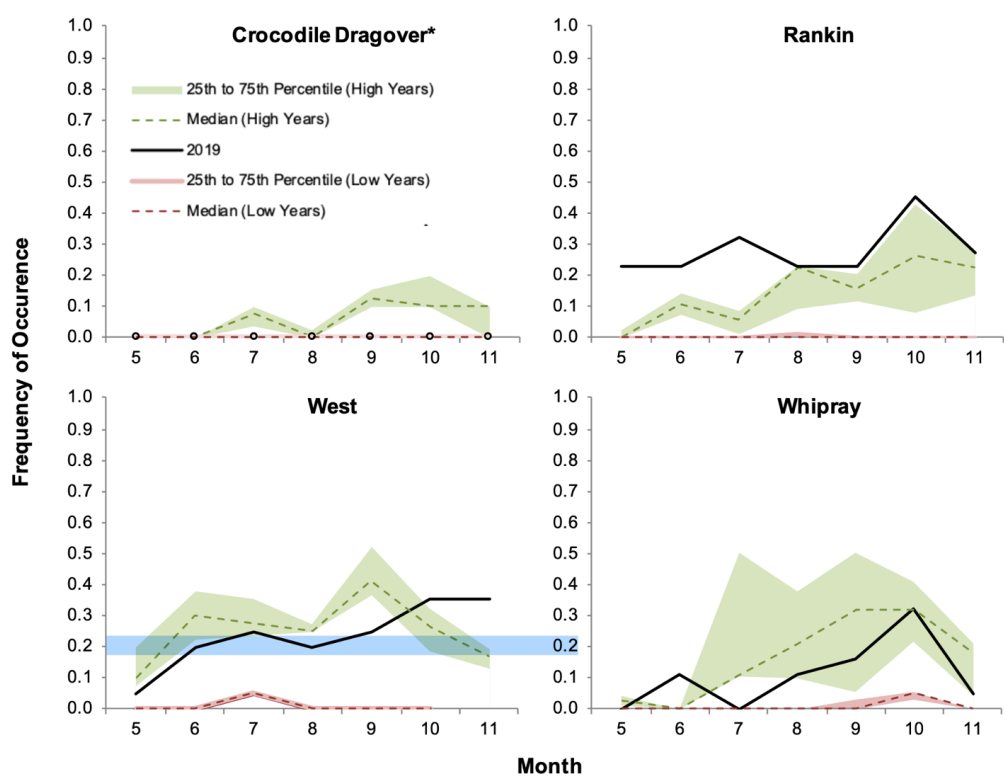
Figure 3. Ribbon plots showing the monthly frequency of occurrence of juvenile *C. nebulosus* within each region for high-population years (shaded in green), low-population years (shaded in red), and 2019 (black). The shading encapsulates the 75th and 25th quartiles of monthly frequency of occurrence for seatrout in high and low years. The black line shows the monthly frequency of occurrence for 2019 (* zero *C. nebulosus* were caught in Crocodile Dragover in 2019, indicated by hollow black points).

Table 2. Spotted seatrout frequency of occurrence for each year and zone from 2004-2019.

| Year	Crocodile	Rankin	West	Whipray	Overall
2004	0.08	0.11	0.10	0.08	0.09
2005	0.11	0.39	0.09	0.15	0.17
2006	0.05	0.23	0.45	0.50	0.34
2007	0.07	0.06	0.15	0.28	0.14
2008	0.00	0.00	0.19	0.02	0.09
2009	0.03	0.01	0.12	0.08	0.06
2010	0.01	0.00	0.19	0.00	0.05
2011	0.00	0.01	0.13	0.01	0.04
2012	0.01	0.00	0.16	0.02	0.05
2013	0.00	0.01	0.12	0.02	0.03
2014	0.00	0.00	0.01	0.01	0.00
2015	0.00	0.00	0.11	0.02	0.03
2016	0.01	0.07	0.24	0.09	0.10
2017	0.02	0.14	0.24	0.05	0.11
2018	0.06	0.21	0.22	0.18	0.17
2019	0.00	0.28	0.24	0.11	0.16
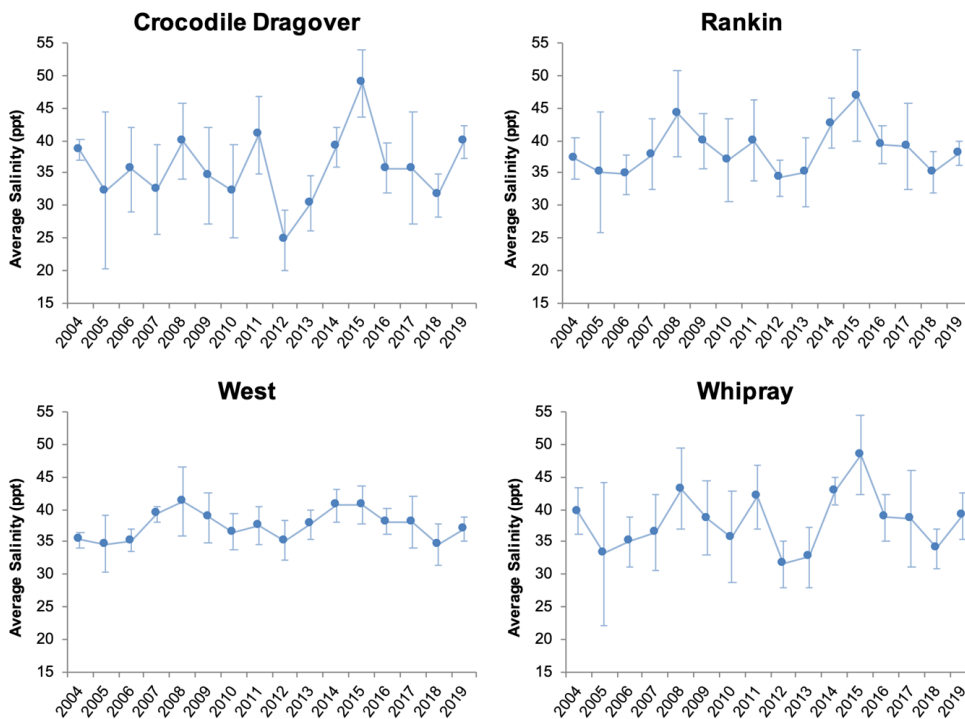
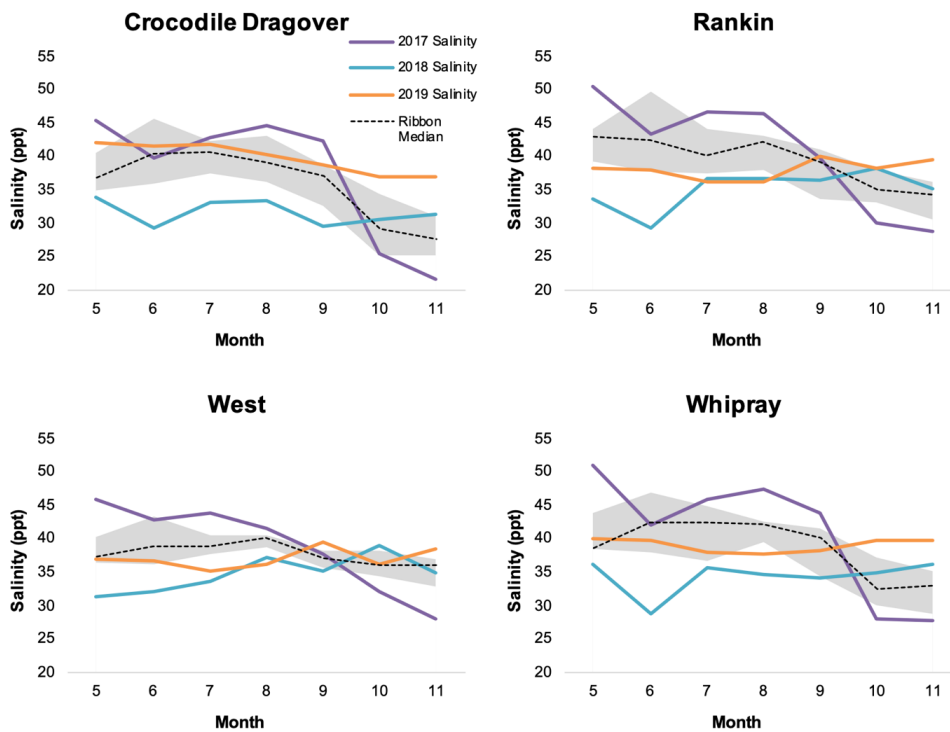**Figure 4. Average salinities and standard deviations at time of tow, by area, and by year.**

Figure 5. Ribbon plots showing the median monthly salinity (ppt) within each region for 2004–2016. The shading encapsulates the 25th to 75th quartiles of the monthly salinities. Purple, blue, and orange lines show the median monthly salinity for 2017, 2018, and 2019, respectively.

In the Whipray Basin sub-region, high-population years of 2004-2007, 2016, 2018, and 2019 had a frequency of occurrence that was at least 8%. Low-population years of 2008 and 2010-2015 had frequency of occurrences of 2% or less. The years 2009 and 2017 were intermediate population years and had frequencies of occurrence of 8% and 5%, respectively. During the initial high-population years of 2004-2007, the peak in juvenile *C. nebulosu*s was observed in the late summer from July through September (**Figure 3**). However, the 2018 and 2019 high-population years, as well as 2016 and 2017, all had peaks later in the season from September through November (**Figure 3**). In the low-population years, no more than two juvenile seatrout were collected each year. In 2006, seatrout were found at 50% of sampled stations (30 stations with juvenile spotted seatrout present out of 60 stations) and, in 2007, seatrout were found at 28% of sampled stations (17 stations with juvenile spotted seatrout present out of 60 stations). In 2019, the Whipray sub-region had a frequency of occurrence of 11% (14 stations with juvenile spotted seatrout present out of 133 stations).

Juvenile spotted seatrout are rarely collected in Crocodile Dragover, an area that represents their easternmost distribution in Florida Bay. Thus, high-population years in Crocodile Dragover in 2004-2007 and 2018 only had a frequency of occurrence of 5% to 11%. Low-population years (2008, 2010-2015, 2019) had a frequency of occurrence of 1% or less. Only five seatrout were collected in Crocodile Dragover in 2016, at just 1% of the stations. In the high-population years, including 2018, juvenile *C. nebulosus* frequencies peaked late in the sampling season from September through November (**Figure 3**). With regard to low-population years, only one seatrout was caught in 2010, one in 2012, and none were caught in 2011, 2013-2015, or 2019. In 2019, in Crocodile Dragover, zero juvenile *C. nebulosus* were caught at any of the stations (out of 140 stations).

Overall, juvenile spotted seatrout populations were low throughout the central bay in 2008 and 2010-2015. The West sub-region has been consistently higher than the central bay except in 2014, the lowest observed population by far in the West (**Figure 2**, **Table 1**). Overall, juvenile spotted seatrout frequency of occurrence varied interannually from 0% in 2014 to 34% in 2006. The results show that there was a statistically significant shift to lower juvenile spotted seatrout populations beginning in 2008 and running through 2015, after which it increased to the third highest overall frequency of occurrence in 2018 (17%) and stayed relatively stable in 2019 (16%) (**Table 2**).

The cause of the shift after 2007 is uncertain, but 2008 had the second highest salinities observed during the MAP sampling period, and 2015 had the highest salinities. These hypersaline periods may have resulted in a shift in seatrout populations. Salinity was lower in 2016 through 2018, and each of the four sub-regions displayed salinity ranges similar to the mid-2000 high population years, which might explain the similarity in densities between those two years (**Figure 4**).

Overall, the highest mean frequency of occurrence of juvenile spotted seatrout throughout Florida Bay since 2007 was found in 2018, meaning that 2018 was a high-population year in all of the sub-regions. In 2019, Rankin and West sub-regions had the highest frequency of occurrence in recent years, and the overall frequency of occurrence remained fairly stable from the previous years. Thus, conditions have improved significantly for juvenile spotted seatrout in the central and western part of Florida Bay since 2016.

3.2 Salinity Patterns during Sampling

Mean salinities in 2019 in each sub-region were 37.0 ± 1.9 in the West, 38.1 ± 1.9 in Rankin, 39.1 ± 3.6 in Whipray, and 39.8 ± 2.6 in Crocodile Dragover. Mean salinities in 2019 were significantly higher than the overall mean salinities for previous years in Crocodile Dragover and significantly lower in the West sub-region than the overall mean salinities for previous years (**Table 3**). All regions showed similar interannual trends in salinity, but the magnitude of variability differed (**Figure 4**).

Mean monthly salinities in the West sub-region display a slight downward trend throughout the sampling season (May–November), but this trend was not as pronounced as in other sub-regions (**Figure 5**). The lowest observed annual mean salinities in the West were during the 2005,

Table 3. Comparison of 2019 salinities by zone to all previous years, including data on the maximum and minimum salinity values recorded for each time period.

Zone	Year	Mean Salinity	Standard Deviation	Maximum	Mininum	p-value
Crocodile Dragover	2004-2018	35.38	8.34	56.20	15.00	0.000*
	2019	39.78	2.56	44.50	34.04	
Rankin	2004-2018	38.77	6.52	64.20	18.75	0.321
	2019	38.05	1.85	41.65	34.75	
West	2004-2018	37.79	3.98	53.00	26.72	0.010*
	2019	37.00	1.94	40.10	22.51	
Whipray	2004-2018	38.18	7.28	65.40	19.00	0.064
	2019	39.08	3.56	44.60	4.30	

*Significant difference between the mean salinity of 2019 versus all other years.

2006, 2012, 2013, and 2018 sampling periods (**Figure 4**). Low salinities were observed in the fall of 2005 and 2017, and the late spring of 2018, following the passage of hurricanes. The two lowest mean monthly salinities were recorded immediately after hurricanes, but the West salinity variability was significantly less than the other regions both interannually and intra-annually (**Figures 4 and 5**), confirming the previously documented influence of Gulf of Mexico waters on western Florida Bay salinity patterns (Kelble *et al.*, 2007). The West sub-region's highest annual mean salinity occurred in 2008 (41.3), followed by 2015 and 2014, with mean salinities greater than 40 in all three years. Salinities in June 2015 were the highest monthly mean observed (44.4) in the West sub-region, and both 2014 and 2015 had hypersaline conditions above the 75th quartile in four of the six months sampled. In 2017, salinity (38.8) was slightly above average. In 2018, salinity (34.7) was significantly lower than average (37.8, p = 0.011). The low salinities early in the 2018 sampling period were likely due to lingering low salinities from the large rains associated with Hurricane Irma, which passed over the study site in September 2017. In 2019, the mean monthly salinity started out below the lower quartile of the historic values, returned within the historic quartile range by September, and was slightly elevated above the upper quartile in November (**Figure 5**).

Rankin experienced similar interannual variability as the West with low annual salinities in 2005, 2006, 2012,

2013, and 2018, and high annual salinities in 2008 (44.1) and 2015 (46.8) (**Figure 4**.). Monthly salinities in this sub-region tend to decline throughout the sampling season (**Figure 5**). As a result, the five lowest monthly mean salinities in this sub-region occurred in the months of October or November. July of 2015 had the highest mean salinity (55.6) in this sub-region, followed by June of 2008 (53.9). Furthermore, every month in 2015 in the Rankin, Whipray, and Crocodile Dragover sub-regions had salinities above the 75th quartile. Salinity in Rankin in 2016 had returned to the historical range at the beginning of the season but was elevated in September and October, and annual mean salinity was still above average and comparable to 2009 and 2011. In 2017, salinities in Rankin started out slightly elevated from baseline conditions before plummeting to significantly below baseline conditions in October and November after the passage of Hurricane Irma. Salinity in Rankin in 2019 was remarkably stable. The year started out with fresher salinities than typical in Rankin, but by September salinities were within and then over the historical quartiles. Mean salinity in 2019 was comparable to the mean salinity of all previous years (**Table 3**).

Whipray had the same interannual patterns in mean salinity as Rankin and Crocodile Dragover, but with higher variability than either sub-region. Whipray had the second highest annual salinity observed (48.24 in 2015), the highest monthly mean salinity on record (57.9 in July

2015), and the highest observed salinity for the entire period of record (65.4), measured during the July 2015 hypersaline event. The lowest annual mean salinities in this sub-region occurred in 2012 and 2013. Monthly salinities in Whipray peaked in the summer from June through August and then decreased for the rest of the sampling period. In 2019, monthly salinities were stable in Whipray, starting out on the low end of the historic quartiles in May and June and finishing on the higher end of historic monthly quartiles in November. The mean salinity in 2019 was comparable to the mean salinity of all previous years (**Table 3**).

Crocodile Dragover had the most variable salinities of any sub-region sampled. This sub-region had the highest overall annual mean salinity (48.75 in 2015) and also the lowest (24.7 in 2012), reflecting the effects of high evaporation coupled with shallow depths, direct freshwater runoff, and poor mixing in the northern interior bay (Lee *et al.*, 2008). In 2019, salinities were stable above the mean of the historic range, rising above the upper quartile by September (**Figure 5**). In fact, the mean annual salinity was significantly higher in 2019 than the overall mean salinity for all previous years by approximately 4 ppt (**Table 3**).

3.3 Spotted Seatrout Distribution and Abundance Relative to Salinity (Potential Restoration Effects)

To examine the impact of salinity on the juvenile spotted seatrout population, data within each sub-region were binned into salinity categories, each with a range of 5 ppt. Bins with five or fewer observations were omitted, due to the inability of such a small sample size to adequately capture the true population dynamics. The data on the seatrout population within each bin were expressed as three abundance metrics: (1) frequency of occurrence (i.e., the percent of tows with at least one juvenile spotted seatrout); (2) the concentration of seatrout only when present (number per 1000 m^{-2}); and (3) density (number per 1000 m^{-2}) for all observations.

Within all of the sub-regions, two or more aspects of the juvenile spotted seatrout population abundance metrics inversely correlated with salinity (**Figure 6**). A decreased frequency of occurrence was significantly correlated

with increasing salinity in Crocodile Dragover, Rankin, and Whipray. Decreasing density was significantly correlated with increasing salinity in Crocodile Dragover, Rankin, and West, while Whipray had the only instance of statistically significant inverse correlation of concentration and salinity (**Figure 6**). However, across all of Florida Bay, salinity did not have an effect on any of the metrics of juvenile spotted seatrout population (**Figure 7**). This indicates that salinity likely does not play a role in shaping the spatial distribution of juvenile spotted seatrout among sub-regions or across the entirety of Florida Bay; however, it does play a major role in driving juvenile spotted seatrout distributions within all of the sub-regions.

3.4 Spotted Seatrout Distribution and Abundance Relative to Seagrass

From 2004 through 2008, seagrass density and biomass were measured. The biomass values were converted to Braun-Blanquet (BB) abundance for years prior to 2009 using a linear regression between biomass and BB abundance. Braun-Blanquet (BB) abundance indices were used directly to quantify seagrass and macroalgae coverage at each station beginning from 2009 to 2012. BB abundance was then converted to percent cover to make the numbers linear and comparable to the percent cover measures, which began in 2013. A linear regression was used again for the years prior to 2009, and a standard conversion was used for the years after 2009. This conversion used the midpoint of percent cover for each BB index score. These indices were measured not only for overall seagrass coverage and algae coverage, but also for each seagrass species (*Thalassia* spp., *Syringodium* spp., and *Halodule* spp.). The average length of each seagrass species was also measured. Seatrout abundance metrics were grouped in bins according to 10% seagrass cover ranges, and the relationship between them is expressed in **Figures 8-11**.

Seagrass has shown significant changes throughout the period of our monitoring. The change that received the most attention was the seagrass die-off that occurred throughout Rankin and in some areas of West and Whipray in September and October 2015 (Hall *et al.*, 2016). Within
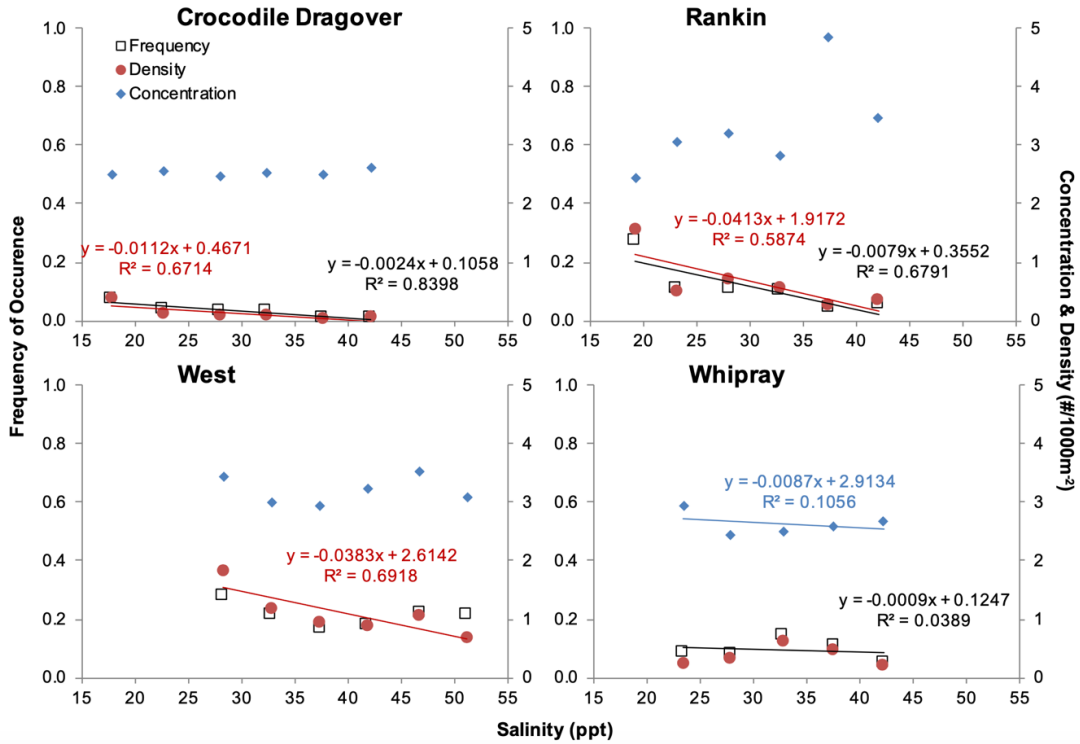
Figure 6. Scatter plots depict the relationship between the juvenile spotted seatrout population and salinity within each sub-region. Black boxes are frequency of occurrence, blue diamonds are concentration, and red circles are density. Only significant linear regressions are depicted.
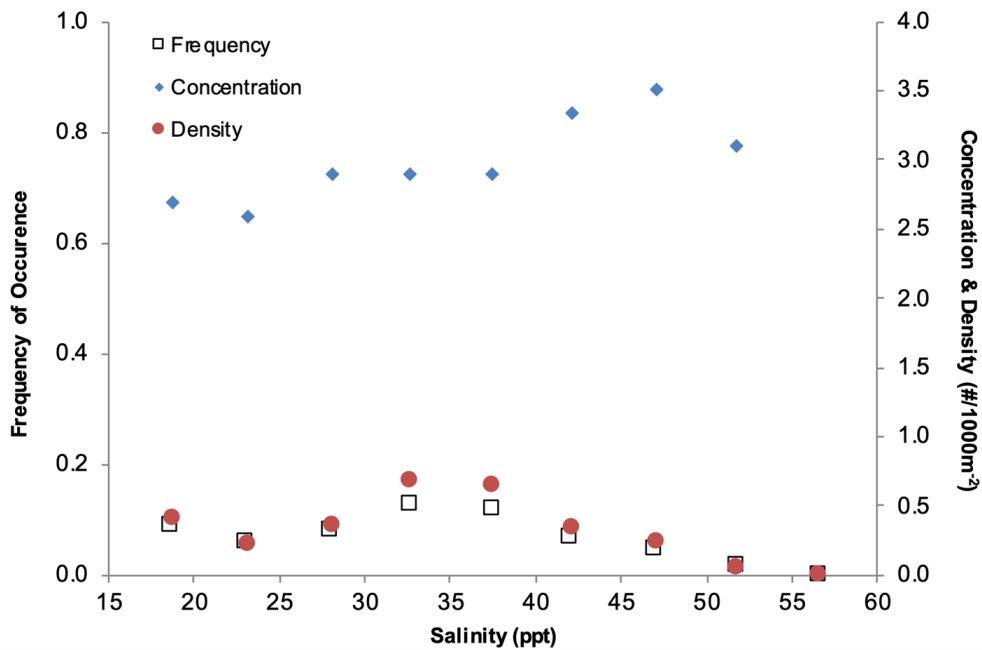

Figure 7. Scatter plot depicts the correlation of the juvenile spotted seatrout population with salinity for all sub-regions combined. The open black boxes are frequency of occurrence, blue diamonds are concentration, and red circles are density. Only significant linear regressions are depicted. Bins have ranges of 5 ppt cover.
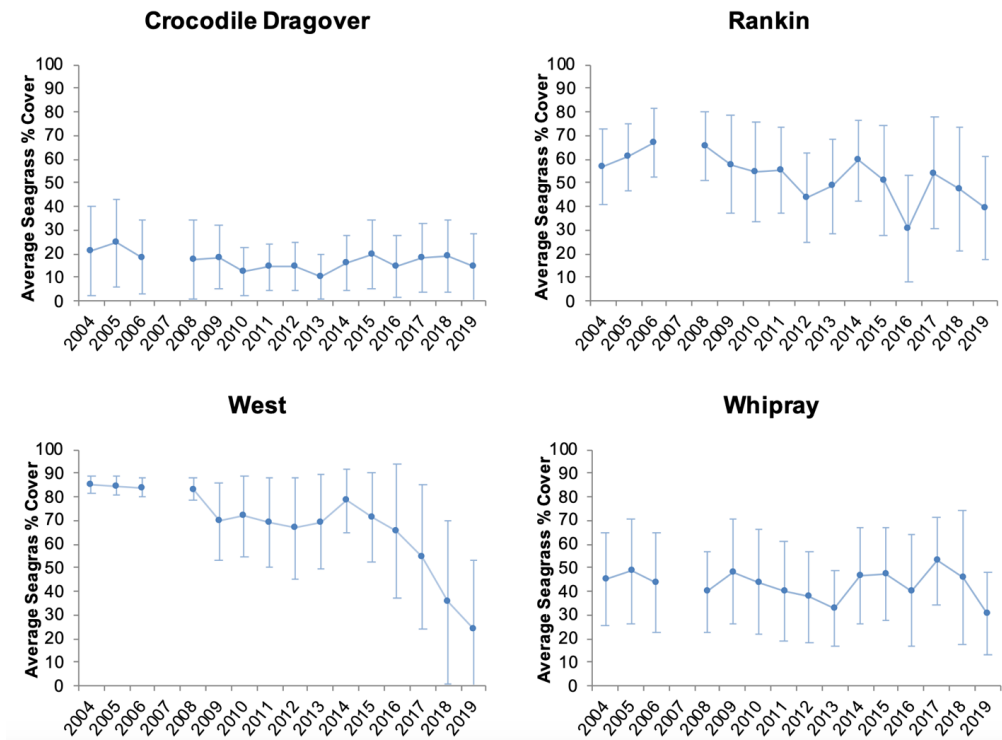
Figure 8. Average seagrass percent cover and standard deviations at time of tow, sub-region, and year.
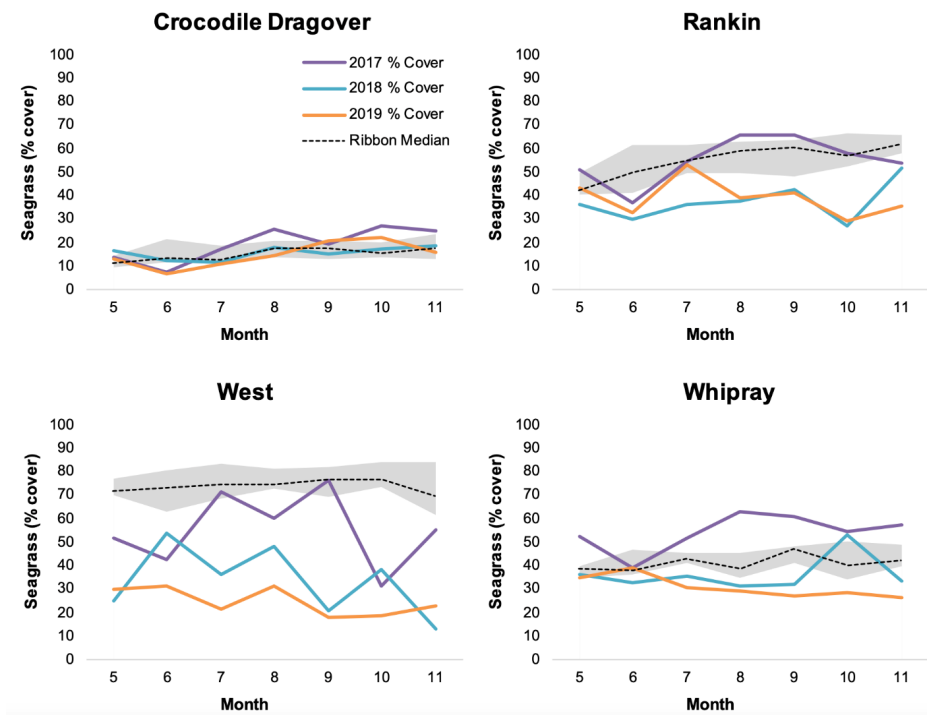

Figure 9. Ribbon plots showing the mean monthly seagrass percent cover within each region for 2004-2016. The shading constrains the 25th to 75th quartiles of monthly seagrass percent cover. The orange, purple, and blue lines show the monthly seagrass percent cover for 2017, 2018, and 2019, respectively.
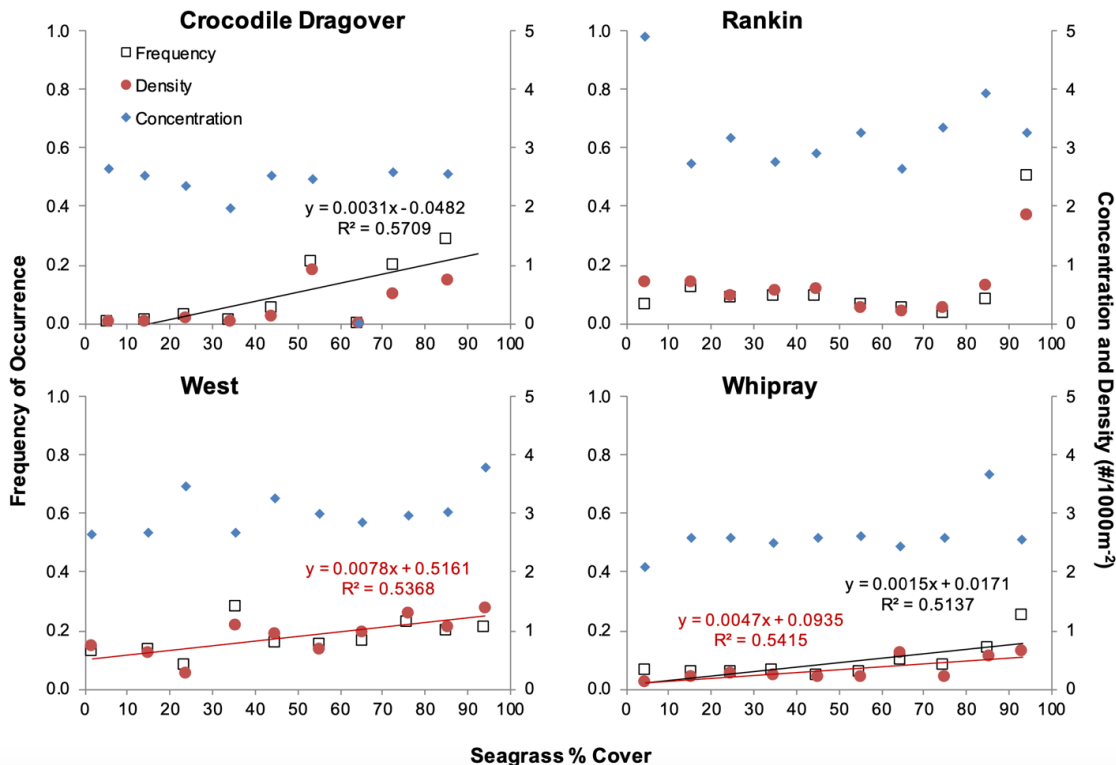
Figure 10. Scatter plots depict the correlation of the juvenile spotted seatrout population with seagrass percent cover for each sub-region. The open black boxes are frequency of occurrence, blue diamonds are concentration, and red circles are density. Only significant linear regressions are depicted.
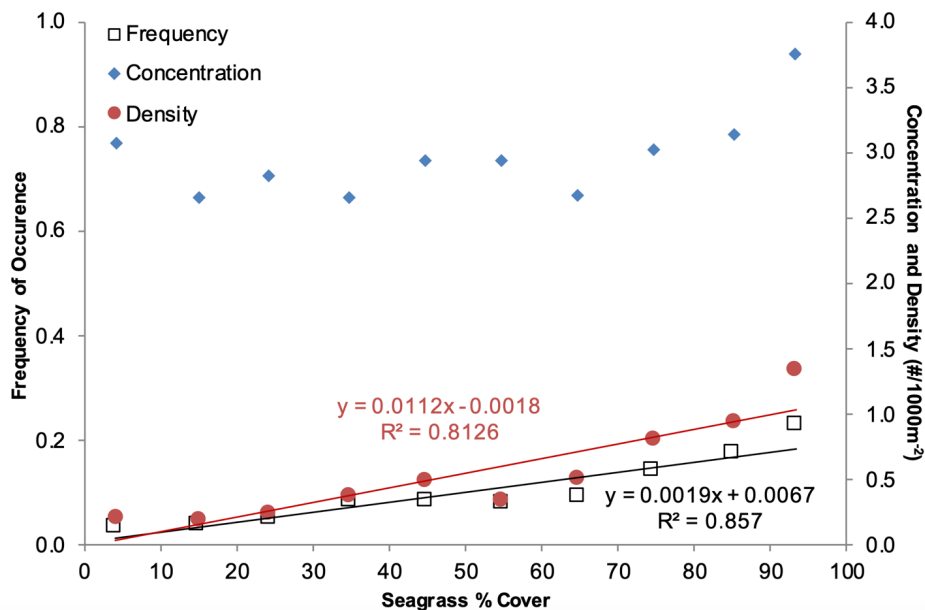

Figure 11. Scatter plot depicts the correlation of the juvenile spotted seatrout population with seagrass percent cover for all sub-regions combined. The open black boxes are frequency of occurrence, blue diamonds are concentration, and red circles are density. Only significant linear regressions are depicted. Bins have ranges of 10% cover.

our dataset, this die-off only produced a significant change in Rankin, as seen by the large decrease in mean monthly seagrass percent cover in Rankin in September and October of 2015. Seagrass percent cover remained low throughout 2016 in Rankin, likely as seagrass was just beginning to recover from the die-off. However, by 2017 seagrass percent cover had returned to its historic range in Rankin. This suggests the recovery, in terms of percent seagrass cover, was less than 2 years in Rankin following a major die-off. Another major signal in the seagrass percent cover data is the steady decrease that has been observed in the West sub-region since 2015. This decrease has been a steady decline in the annual mean since 2015 with a corresponding increase in the standard deviation. This decline persisted in 2019 and all sub-regions reported lower than average seagrass percent cover density this year (**Figure 9**).

When separated by sub-region (**Figure 10**), the relationship between seagrass percent cover and juvenile spotted seatrout shows some differences. However, when looking at all regions together, there is a significant positive linear relationship between seagrass percent cover and spotted seatrout density (p < 0.001) and frequency of occurrence (p < 0.001) (**Figure 11**). In Rankin, there were no significant linear regressions with density, frequency of occurrence, or concentration to seagrass percent cover. In Crocodile Dragover, only frequency of occurrence was significantly correlated with seagrass percent cover (p < 0.019). In West, only density was significantly correlated with seagrass percent cover (p < 0.016). Lastly, in Whipray both density and frequency of occurrence were significantly correlated with seagrass percent cover (p < 0.015 and p < 0.020, respectively). This suggests that, as percent cover increases, juvenile spotted seatrout are caught more frequently in all regions except Rankin. Moreover, it suggests that seagrass may play a larger role in shaping bay-wide (i.e., among sub-regions) distributional differences in *C. nebulosus* since bay-wide regressions are significant for both frequency of occurrence and density (**Figure 11**).

3.5 Spotted Seatrout Distribution and Abundance Relative to Temperature

To examine the impact of temperature on the juvenile spotted seatrout population, data were binned into temperature categories, each with a range of 2° Celsius. Bins with five or fewer observations were omitted due to the inability of such a small sample size to adequately capture the true population dynamics. The data on the seatrout population were expressed as three abundance metrics: (1) frequency of occurrence (i.e., the percent of tows with at least one juvenile spotted seatrout); (2) the concentration of seatrout only when present (number per 1000 m^{-2}); and (3) density (number per 1000 m^{-2}) for all observations.

In 2019, the annual mean temperature for all sub-regions was higher than the previous years but, when comparing 2019 to all previous years, only Whipray and Crocodile Dragover were significantly higher (p < 0.038 and p < 0.000 respectively) (**Figure 12**, **Table 4**). Otherwise, there were no significant linear relationships of any abundance metric with temperature (**Figure 13**). Although the relationship is parabolic in nature, no obvious parabolic relationships were noted. Because the relationship between temperature and seatrout populations in this region is non-linear, we used a logistic regression to identify the relationship between salinity, temperature, seagrass percent cover, and seatrout frequency of occurrence. There were no relationships with temperature when all of the data across all regions was pooled (**Figure 14**). This suggests that temperature is currently having little effect on juvenile spotted seatrout population distributions in Florida Bay.

3.6 Spotted Seatrout Diet based on Stomach Cultures

We examined the stomach contents of 976 spotted seatrout <100 mm standard length caught from 2010–2019. The results are grouped by the total biomass of each phylogenetic group found in the stomach (**Figure 15**). The three most abundant prey items found in the stomach were shrimp from the infraorder *Caridea*, shrimp from the Family *Penaeidae*, and fish from the Family *Fundulidae*. Among 16 other groupings of prey items,
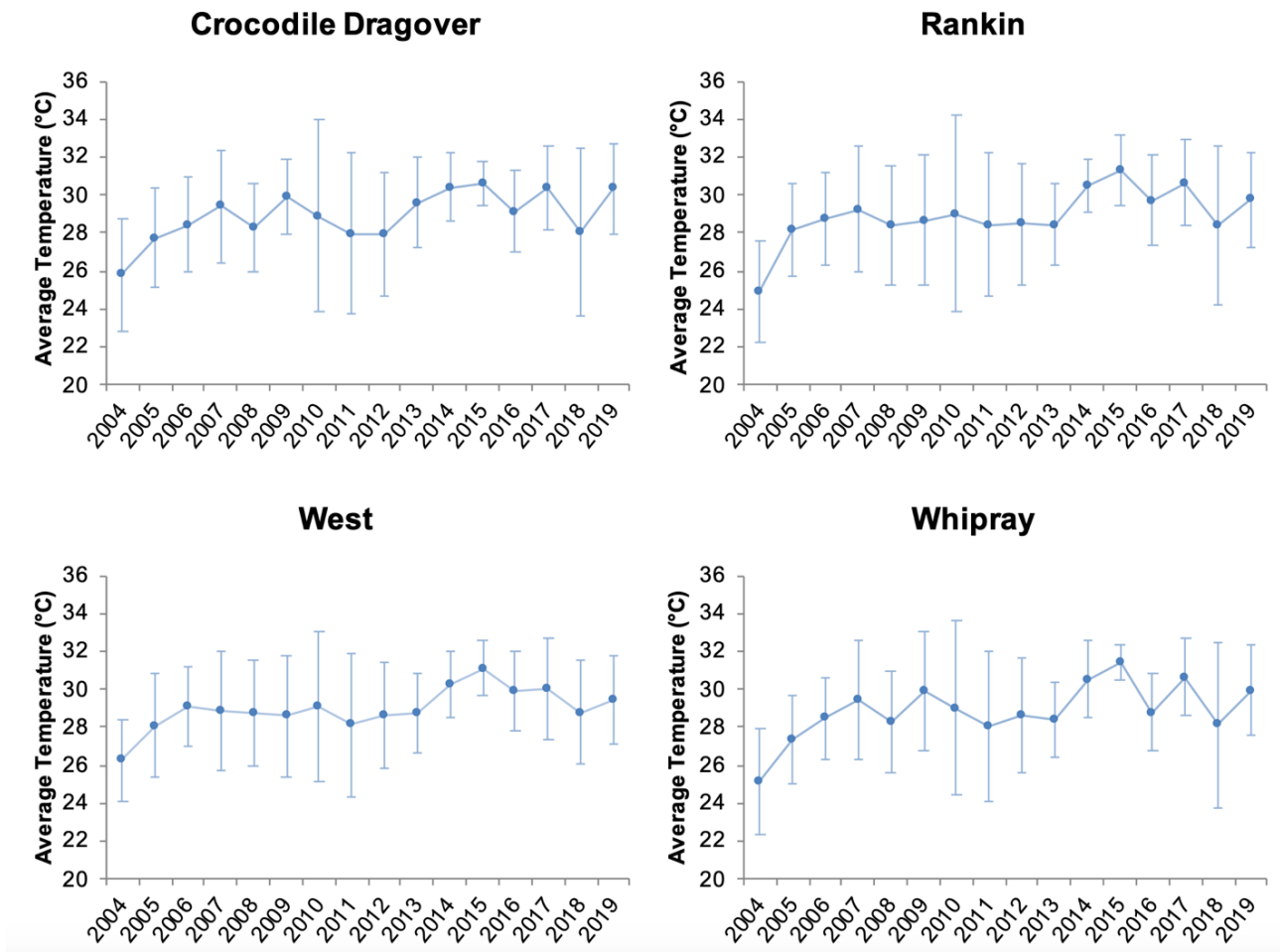
Crocodile Dragover

Rankin

West

Whipray

Figure 12. Average temperature and standard deviations at time of tow, by area, and by year.

Table 4. Comparison of 2019 temperatures by zone to all previous years, including data on the maximum and minimum salinity values recorded for each time period.

Zone	Year	Mean Temperature	Standard Deviation	Maximum	Mininum	p-value
Crocodile Dragover	2004-2018	29.07	3.26	39.40	17.09	0.000*
	2019	30.33	2.41	39.99	25.08	
Rankin	2004-2018	29.12	3.38	38.00	13.33	0.947
	2019	29.77	2.50	39.79	24.49	
West	2004-2018	29.06	2.90	43.00	15.47	0.455
	2019	29.44	2.35	35.55	20.20	
Whipray	2004-2018	29.11	3.25	42.60	15.49	0.038*
	2019	29.94	2.37	35.53	24.96	

*Significant difference between the mean temperature of 2019 versus all other years.
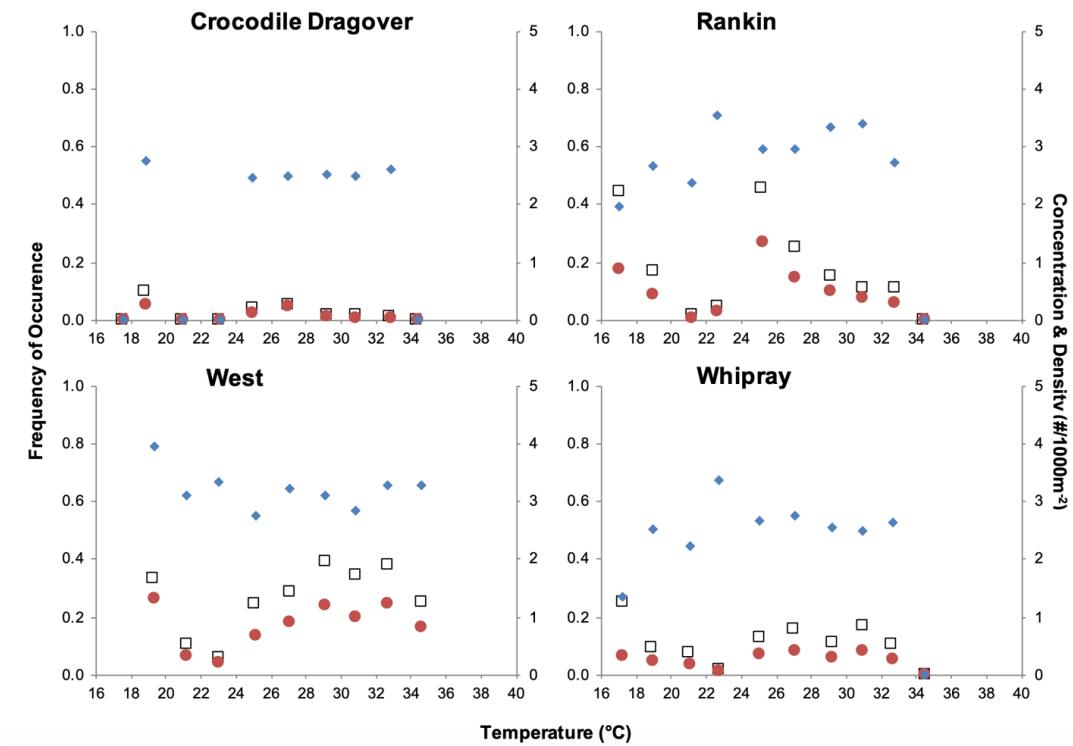
Figure 13. Scatter plots depict the correlation of the juvenile spotted seatrout population with temperature for each sub-region. The open black boxes are frequency of occurrence, blue diamonds are concentration, and red circles are density. Only significant regressions are depicted.
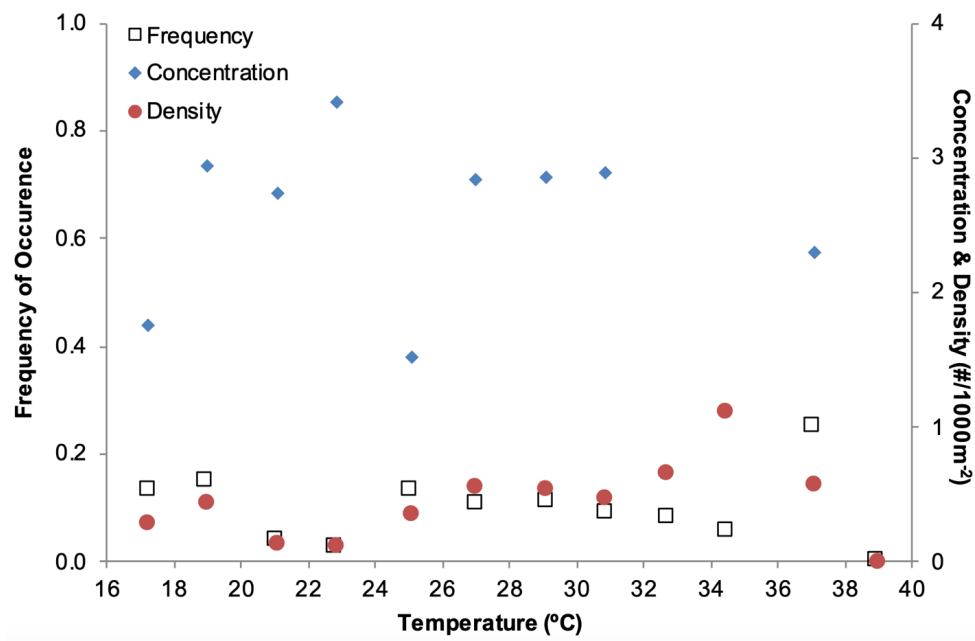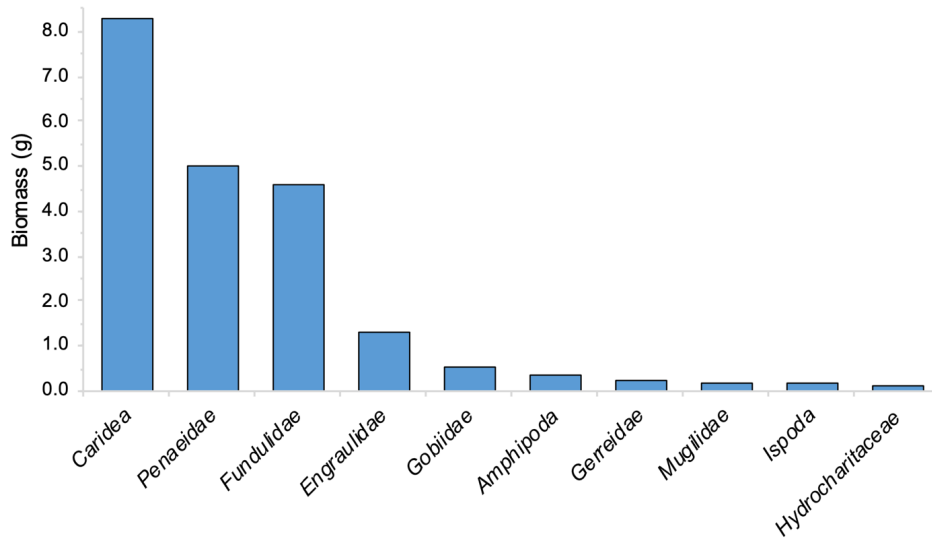

Figure 14. Scatter plot depicts the correlation of the juvenile spotted seatrout population with temperature for all sub-regions combined. The open black boxes are frequency of occurrence, blue diamonds are concentration, and red circles are density. Bins have ranges of 2°C.

Figure 15. Total biomass (g) of stomach contents from 976 spotted seatrout (<100 mm standard length) caught from 2010-2019 shown by phylogenetic grouping.

anchovies (*Anchoa* and *Engraulidae*), gobies (*Gobiidae*), crustaceans of the order *Amphipoda*, *Mojarra* (*Gerreidae*), and mullet (*Mugliidae*) were the next most abundant in biomass. When the top three prey item categories were analyzed by month, it was observed that juvenile seatrout feed primarily on organisms from the *Penaidae* and *Fundulidae* families from May until August, when they then switch to primarily eating organisms in the *Caridea* infraorder (**Figure 16**).

3.7 Juvenile *C. nebulosus* Performance Measure Development

A performance measure for juvenile spotted seatrout was accepted for use in July 2017. It has already been applied to evaluate the potential effect of Central Everglades Planning Project alternatives and the likely impact of future climate change scenarios (Kelble *et al.*, 2007; Kearney *et al.*, 2015).

3.8 Relationship of Other Sportfish to Salinity

Beginning in 2009, we expanded the project to collect information on other sportfish species within Florida Bay. Thus, we have ten years of information for many of these species. However, a smaller subset of these species has been enumerated since MAP sampling began in 2004

(**Table 5**). Florida stone crab and Atlantic blue crab have been caught regularly since 2018 and, as such, we have included their numbers in the table. We investigated the relationship of species richness (number of species per tow) for several common sportfishes to their salinity preferences (**Figure 17**).

The richness of sportfish taxa (defined by **Table 5**) observed in the bay showed a significant dependence on salinity (**Figure 17**). The tows in which no sportfish were observed had significantly higher salinities (mean = 38.1, lower quartile = 33.9, upper quartile = 42.5, p < 0.001) than the overall salinity distribution (mean = 37.7, lower quartile = 34.1, upper quartile = 41.3). Stations where one (mean = 36.6, p < 0.001), two (mean = 36.9, p < 0.001), or three (mean = 36.8, p < 0.001) sportfish taxa were observed had significantly lower salinities than stations where no sportfish were observed. Salinities for stations with four, five, and six taxa represented in a tow were not significantly different from the overall salinity distribution. Due to the low sample size (n <10) for stations with seven or more taxa represented in a tow, these were not analyzed for significance.

Salinity preferences of each sportfish taxa contribute to the overall diversity and can also contribute to the temporal and spatial distribution of the taxa. To examine
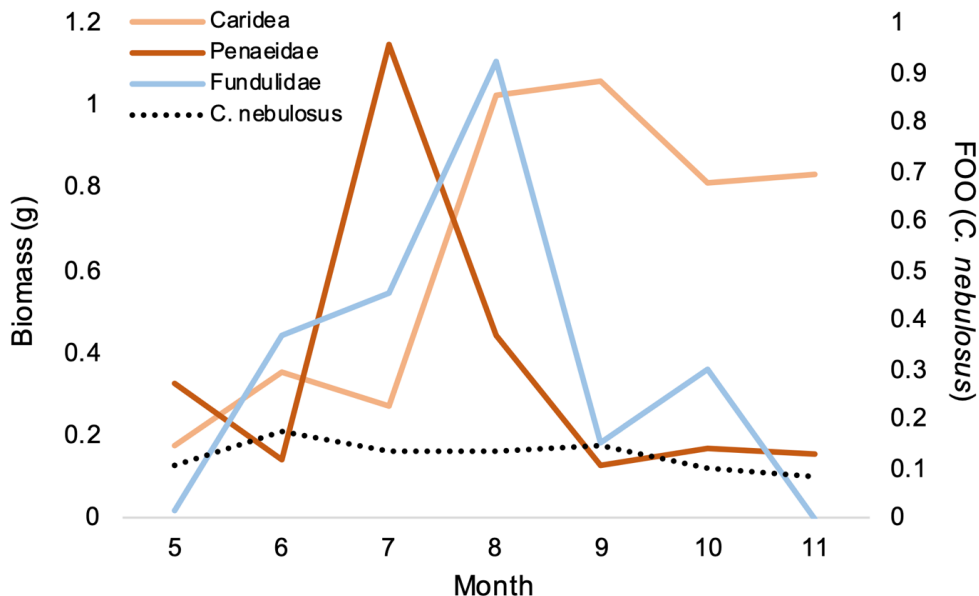
Figure 16. Monthly total biomass (g) of the three most abundant prey groups (solid lines) found in juvenile spotted seatrout stomach content from 2004–2019, and seatrout frequency of occurrence (dotted line) at collection stations.
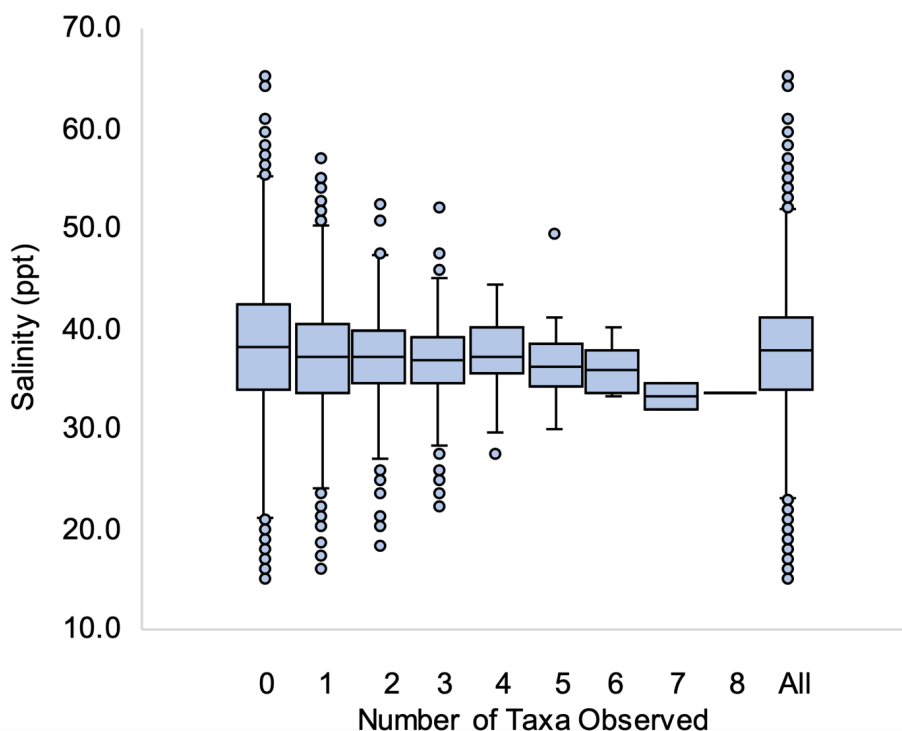
Figure 17. Box and whisker plot depicting the salinity range for the number of sportfish taxa observed in a tow (e.g., the second box and whisker plot from the left depicts the salinity range for tows where zero of the 25 sportfish taxa were observed). Data includes all MAP observations (2004-2019). All Values is the range of all salinity values observed. The central line is the median, the box depicts the range of 25th to 75th quartiles, the whiskers demark the minimum and maximum of non-outlier values, and the circles depict the outliers.

Table 5. Salinity ranges and means with 95% confidence intervals and site sample size (n) for the 25 species that have been enumerated since the project's inception in 2004.

Code	Species Name	Common Name	Salinity Range	Mean ± std	n
Ari	*Argopecten irradians*	Atlantic Bay Scallop	18.0 - 52.5	37.6 ± 4.91	1555
Arp	*Archosargus probatocephalus*	Sheepshead	25.0 - 51.2	38.1 ± 4.00	157
Bab	*Bairdiella batabana*	Blue Croaker	30.1 - 39.4	34.7 ± 2.42	30
Chf	*Chaetodipterus faber*	Atlantic Spadefish	25.0 - 47.0	35.7 ± 3.84	103
Cyn	*Cynoscion nebulosus*	Spotted Seatrout	16.0 - 52.5	36.3 ± 4.98	1474
Epi	*Epinephelus itajara*	Goliath Grouper	35.3 - 44.5	38.7 ± 3.30	7
Has	*Haemulon sciurus*	Bluestriped Grunt	23.5 - 45.0	36.4 ± 3.69	163
Hie	*Hippocampus erectus*	Lined Seahorse	23.9 - 57.0	38.9 ± 5.39	226
Hpa	*Haemulon parra*	Sailor's Grunt	31.2 - 40.4	35.2 ± 3.38	7
Hyp	*Hypoplectrus unicolor*	Butter Hamlet	26.5 - 40.3	35.5 ± 2.25	85
Lam	*Lachnolaimus maximus*	Hogfish	30.0 - 49.4	38.2 ± 3.54	166
Lug	*Lutjanus griseus*	Gray Snapper	18.4 - 55.5	36.8 ± 4.53	3460
Lum	*Lutjanus mahogani*	Mahogany Snapper	31.4 - 40.8	37.4 ± 3.09	20
Lun	*Lutjanus analis*	Mutton Snapper	30.2 - 44.0	37.3 ± 4.73	16
Lus	*Lutjanus synagris*	Lane Snapper	22.5 - 53.0	37.0 ± 4.08	4447
Mym	*Mycteroperca microlepis*	Gag Grouper	28.5 - 44.0	36.4 ± 3.20	23
Occ	*Ocyurus chrysurus*	Yellowtail Snapper	22.5 - 49.4	37.2 ± 5.19	74
Paa	*Panulirus argus*	Caribbean Spiny Lobster	29.7 - 52.0	38.2 ± 4.93	82
Pab	*Paralichthys albigutta*	Gulf Flounder	29.0 - 43.2	35.7 ± 4.41	9
Pal	*Paralichthys lethostigma*	Southern Flounder	33.3 - 40.4	36.7 ± 2.31	12
Poc	*Pogonias cromis*	Black Drum	22.3 - 42.7	32.9 ± 7.62	5
Scb	*Scorpaena brasiliensis*	Barbfish	28.7 - 42.6	35.4 ± 3.85	17
Sco	*Sciaenops occelatus*	Redfish	30.5 - 36.8	34.6 ± 2.71	6
Sev	*Selene vomer*	Lookdown	27.4 - 44.5	37.0 ± 5.24	11
Spa	*Syphyraena barracuda*	Great Barracuda	18.4 - 55.6	36.8 ± 6.36	953
Mem	*Menippe mercenaria*	Florida Stone Crab	31.8 - 39.3	35.7 ± 2.85	7
Cas	*Callinectes sapidus*	Atlantic Blue Crab	22.5 - 39.2	33.5 ± 3.67	132

species salinity preference, we used a subset of the sportfish taxa presented in **Table 5** that focused on nine species with larger sample sizes and economic relevance. Not only were there significant differences in salinities where these taxa were present (**Figure 17**), but there were also significant distribution patterns (**Figure 18**). First, the upper quartile for salinity distributions of all taxa was less than the upper quartile for all salinity values, despite the approximately one order of magnitude larger sample size for all salinity values. This large sample size would constrict the quartile range, suggesting that these taxa are less commonly found in hypersaline conditions. Moreover, five taxa (Atlantic spadefish, spotted seatrout, grey snapper, lane snapper, and great barracuda) had salinity distributions that were significantly ($\alpha = 0.05$)

less than the overall salinity distribution (**Figure 18**). This suggests that if CERP is successful at mitigating hypersalinity, these taxa should become more common. Additionally, Atlantic blue crab had a salinity distribution that was significantly lower than that of all other sportfish species ($p < 0.000$), suggesting that hyposaline conditions favor crab presence in the bay (**Figure 18**).

4. Lessons Learned

The development of a *Cassiopeia* bloom after the seagrass die-off is difficult to impossible to analyze because we were not systematically recording observations of *Cassiopeia*. This led us to re-examine the way we measured the benthic habitat associated with our data collections. In 2016, we
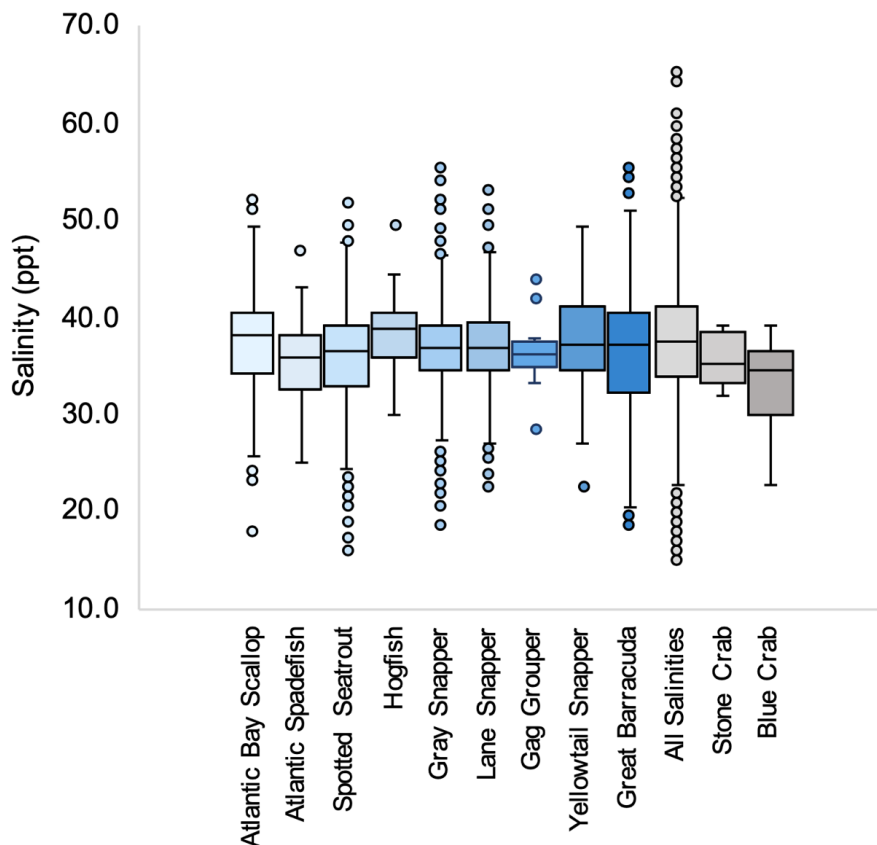
Figure 18. Box and whisker plot depicting the range of salinity values within which the identified sportfish species was observed. Data includes all MAP observations (2004-2019). The central line is the median, the box depicts the range of the lower to upper quartile, the whiskers demark the minimum and maximum of non-outlier values, and circles depict the outliers. Stone crab and blue crab data were collected at each station beginning in 2018.

began to measure biovolumes of *Cassiopeia*. In 2017, we attempted to measure seagrass and benthic habitat by taking continuous pictures of the bottom as we towed, but the camera apparatus suffered a severe malfunction and was not fixed during our sampling season. We have now operationalized a new camera system since the 2018 season and look forward to continued use of the camera to the verify accuracy of seagrass cover data collection. We will then create a mosaic of the area we towed from these pictures and analyze these images to calculate seagrass and macroalgal percent cover and *Cassiopeia* coverage.

We optimized our sampling protocol based upon the results of the first ten years of sampling and the power analyses. The power analyses results suggested we collect the

following number of samples per year in each sub-region: 90 samples in West, 138 samples in Rankin, 114 samples in Whipray, and 120 samples in Crocodile Dragover. However, we were uncomfortable with the dramatic reduction in sampling effort (from approximately 150) for the West sub-region where the juvenile spotted seatrout population is mainly concentrated but highly variable. Therefore, starting in 2009, we collected 120 samples in the West sub-region, 138 samples in Rankin, 114 samples in Whipray, and 120 samples in Crocodile Dragover. This new sampling regime required the collection of 492 samples per year, up 132 samples from the old sampling regime. In 2011, we began collecting 140 samples in the West sub-region, 152 in Rankin, 134 in Whipray, and 140 in Crocodile Dragover for a total of 566 samples per

year. This new sampling regime improved our ability to estimate the juvenile spotted seatrout population in the central areas of the bay, where the population is often low, but where the greatest changes from CERP may occur.

To allow for this expansion in juvenile spotted seatrout sampling without increased cost, we altered the methodology for collecting seagrass data. The general linear model (GLM) analysis showed only a minor dependency on seagrass, and this occurred when seagrass biomass increased to at least its 25th quartile. The only significant effect of seagrass appears to be when seagrass is sparse or non-existent, which reduces the concentration of juvenile spotted seatrout. Based upon this finding, we sampled seagrass via estimation of Braun-Blanquet abundance of each species using a 0.5 m^2 quadrat at nine points along the towline. This sampling methodology will likely still allow for the determination of seagrass and macroalgal abundance at the resolution necessary to examine and account for its effect on juvenile spotted seatrout. Furthermore, this methodology improves the disparity between sampling scales by two orders of magnitude for the trawl and seagrass sampling. To more accurately analyze seagrass abundance and its relationship to juvenile spotted seatrout abundance, starting in 2014 we recorded seagrass percent cover per quadrat directly instead of Braun-Blanquet abundance. This is because the abundance/dominance scores fall on an ordinal scale, and typical statistical methods cannot be properly employed (Podani, 2006). Previous Braun-Blanquet scores were converted to percent cover for this analysis, and percent cover will be recorded directly moving forward.

In 2011, we began our sampling season in May, one month earlier, because our data for subsequent months suggested we were not accurately capturing the onset of the juvenile *C. nebulosus* abundance peak, particularly in the West sub-region (**Figure 5**). We continued the May sampling beyond the 1-year trial in 2011 because we observed a high frequency of occurrence of juvenile *C. nebulosus* in the West sub-region that year. In 2013, we sampled in April as another trial but captured no seatrout and so resumed the May start month in 2014. In 2018, we sampled in January and March to observe the latent effects of Hurricane Irma on juvenile seatrout and since then have extended our sampling season to also include bi-monthly sampling outside of the regular May through November field season (Zink *et al.*, 2020).

Our analyses this year with our new water-quality-model-based hyperspectral imaging (HSI) confirmed that simulated natural system model (NSM) conditions provide a sound restoration target for juvenile spotted seatrout abundance in each of our Florida Bay sampling sub-regions. Furthermore, the HSI model sufficiently discriminated between alternatives of the Central Everglades Project design and future without CERP, with regards to differences in juvenile spotted seatrout abundances. The next steps for the model now that we have several years of data is to recalibrate the model from collected data to further improve its ability to simulate conditions for juvenile spotted seatrout in Florida Bay.

5. References

Chester, A.J., and G.W. Thayer, 1990: Distribution of spotted seatrout (*Cynoscion nebulosus*) and gray snapper (*Lutjanus griseus*) juveniles in seagrass habitats of western Florida Bay. *Bulletin of Marine Science*, 46(2):345–357.

Cohen, J., 1988: *Statistical Power Analysis for the Behavioral Sciences,* 2nd edition. Lawrence Erlbaum Associates Inc., Mahwah, NJ, 567 pp.

Fourqurean, J.W., and M.B. Robblee, 1999: Florida Bay: A history of recent ecological changes. *Estuaries,* 22:345–347, https://doi.org/10.2307/1353203.

Hall, M.O., B.T. Furman, M. Merello, and M.J. Durako, 2016: Recurrence of *Thalassia testudinum* seagrass die-off in Florida Bay, USA: Initial observations. *Marine Ecology Progress Series*, 560:243–249, https://doi.org/10.3354/meps11923.

Kearney, K.A., M. Butler, R. Glazer, C.R. Kelble, J.E. Serafy, and E. Stabenau, 2015: Quantifying Florida Bay habitat suitability for fishes and invertebrates under climate change scenarios. *Environmental Management*, 55(4):836–856, https://doi.org/10.1007/s00267-014-0336-5.

Kelble, C.R., E.M. Johns, W.K. Nuttle, T.N. Lee, R.H. Smith, and P.B. Ortner, 2007: Salinity patterns of Florida Bay. *Estuarine Coastal and Shelf Science,* 71(1-2):318–334, https://doi.org/10.1016/j.ecss.2006.08.006.

Lee, T.N., N. Melo, E. Johns, C. Kelble, R.H. Smith, and P. Ortner, 2008: On water renewal and salinity variability in the northeast sub-region of Florida Bay. *Bulletin of Marine Science,* 82(1): 83–105.

Orlando, S.P., Jr., M.B. Robblee, and C.J. Klein, 1997: Salinity characteristics of Florida Bay: A review of the archived data set (1955-1995). NOAA-Office of Ocean Resources Conservation and Assessments, Silver Spring, Maryland, 33 pp.

Podani, J., 2006: Braun-Blanquet's legacy and data analysis in vegetation science. *Journal of Vegetation Science,* 17(1):113–117, https://doi.org/10.1111/j.1654-1103.2006.tb02429.x.

Powell, A.B., 2003: Larval abundance and distribution, and spawning habits of spotted seatrout, *Cynoscion nebulosus*, in Florida Bay, Everglades National Park, Florida. *Fisheries Bulletin*, 101:704–711, http://aquaticcommons.org/id/eprint/15160.

Powell, A.B., G.W. Thayer, M. Lacroix, and R. Cheshire, 2007: Juvenile and small resident fishes of Florida Bay, a critical habitat in the Everglades National Park, Florida. NOAA Professional Paper NMFS 6, 210 pp.

Rutherford, E.S., T.W. Schmidt, and J.T. Tilmant, 1989: Early life history of spotted seatrout (*Cynoscion nebulosus*) and gray snapper (*Lutjanus griseus*) in Florida Bay, Everglades National Park, Florida. *Bulletin of Marine Science,* 44(1):49–64.

Sokal, R.R., and F.J. Rohlf, 1981: *Biometry: The Principles and Practice of Statistics in Biological Research,* 2nd edition. W.H. Freeman & Company, San Francisco, CA, 859 pp.

Thayer, G.W., and A.J. Chester, 1989: Distribution and abundance of fishes among basin and channel habitats in Florida Bay. *Bulletin of Marine Science,* 44(1):200–219.

Thayer, G.W., W.F. Hettler, Jr., A.J. Chester, D.R. Colby, and P.J. McElhaney, 1987: Distribution and abundance of fish communities among selected estuarine and marine habitats in Everglades National Park. South Florida Research Center Rep. SFRC-87/02. Everglades National Park, South Florida Research Center, Homestead, Florida.

Thayer, G.W., A.B. Powell, and D.E. Hoss, 1999: Composition of larval, juvenile, and small adult fishes relative to changes in environmental conditions in Florida Bay. *Estuaries,* 22:518–533, https://doi.org/10.2307/1353215.

Zieman, J.C., J.W. Fourqurean, and R.L. Iverson, 1989: Distribution, abundance and productivity of seagrasses and macroalgae in Florida Bay. *Bulletin of Marine Science,* 44(1):292–311.

Zink, I.C., J.A. Browder, C.R. Kelble, E. Stabenau, C. Kavanagh, and Z.W. Fratto, 2020: Hurricane-mediated shifts in a subtropical seagrass associated fish and macroinvertebrate community. *Estuaries and Coasts,* 43:1174–1193, https://doi.org/10.1007/s12237-020-00715-2.

National Oceanic and Atmospheric Administration

OFFICE OF OCEANIC AND ATMOSPHERIC RESEARCH
Atlantic Oceanographic and Meteorological Laboratory
4301 Rickenbacker Causeway
Miami, FL 33149

www.aoml.noaa.gov